Sonosensitive theranostic liposomes for preclinical in vivo MRI-guided visualization of doxorubicin release stimulated by pulsed low intensity non-focused ultrasound

Elsevier Editorial System(tm) for Journal of Controlled Release
Manuscript Draft

Manuscript Number:

Title: Preclinical in vivo MRI-guided visualization of Doxorubicin release from liposomes stimulated by pulsed low intensity non-focused Ultrasound

Article Type: Research Paper

Section/Category: Nanomedicine

Keywords: Theranosis, MRI, Liposomes, Ultrasound, controlled drug release

Corresponding Author: Dr. Silvia Rizzitelli, Ph.D.

Corresponding Author's Institution: University of Torino

First Author: Silvia Rizzitelli, Ph.D.

Order of Authors: Silvia Rizzitelli, Ph.D.; Pierangela Giustetto, MSc.; Juan C Cutrin, Ph.D.; Daniela Delli Castelli, Ph.D.; Cinzia Boffa, MSc.; Marta Ruzza, MSc.; Valeria Menchise, Ph.D.; Filippo Molinari, Ph.D.; Silvio Aime, Ph.D.; Enzo Terreno, Ph.D.

Abstract: The theranostic properties of a liposome containing Gadoteridol as MRI reporter and Doxorubicin have been assessed. The release of the drug and the contrast agent is triggered by the application of pulsed Low Intensity Non Focused Ultrasound (pLINFU). The theranostic system has been first characterized in vitro. Then, it has been tested in vivo on a syngeneic murine model of TS/A breast cancer. MRI offered an excellent guidance for monitoring the pLINFU-stimulated release of the drug by providing: i) an in vivo proof of the effective release of the liposomal content, and ii) an assessment of the therapeutic benefits of the overall protocol. Ex vivo fluorescence microscopy indicated that the good therapeutic outcome was originated from an improved diffusion of the drug in the tumor following the pLINFU stimulus. It has been found that the good diffusion of the drug in the tumor stroma is associated with the extravasation/accumulation of the liposomes in the tumor region. The theranostic agent herein developed has a high clinical translatability because the used liposomes, Doxorubicin, and MRI agent are entities already approved for human use.

Suggested Reviewers: Gerben Koning
Laboratory Experimental Surgical Oncology, Erasmus Mc, Rotterdam
g.koning@erasmusmc.nl
Expert in development and application of lipid-based nanocarriers for drug delivery, molecular imaging and imaging-guided drug delivery

Twan Lammers
Experimental Molecular Imaging (ExMI), Aachen
tlammers@ukaachen.de
Expert in drug targeting to tumors, image-guided drug delivery and tumor-targeted combination therapies

David Needham
Mechanical Engineering and Materials Science, Duke University

d.needham@duke.edu

Department of Molecular Biotechnology & Health Sciences
University of Torino

Prof. Enzo Terreno
Molecular & Preclinical Centers
Department of Molecular Biotechnology & Health Sciences
University of Torino
Via Nizza, 52
10126 – Torino, Italy
Phone: +39-011-6706452
Fax: +39-011-6706487
e-mail: enzo.terreno@unito.it

Torino, July 31th, 2014

Dear Editor,

The manuscript entitled "*Preclinical in vivo MRI-guided visualization of Doxorubicin release from liposomes stimulated by pulsed low intensity non-focused Ultrasound*" authored by Silvia Rizzitelli, Pierangela Giustetto, Juan C. Cutrin, Daniela Delli Castelli, Cinzia Boffa, Marta Ruzza, Valeria Menchise, Filippo Molinari, Silvio Aime and myself has been submitted as a full paper to *Journal of Controlled Release* for your consideration.

This study demonstrated that MRI can successfully guide the intratumor release of Doxorubicin from liposomes stimulated by the local application of pulsed Low Intensity Non Focused Ultrasound. The method relies on the encapsulation of the clinically approved MRI agent Gadoteridol in liposomes already used in clinical chemotherapy.

This procedure may provide an efficient imaging tool to monitor the effective release of the drug in vivo on a personalized base. The investigated theranostic agent has a high clinical translatability. Additionally, the US stimulation led to a significant benefit in the therapeutic outcome of the proposed nanomedicine, when compared with the pharmacological results in the non-stimulated procedure.

We hope that this study will be of interest for the audience of the Journal.

Yours sincerely,

Enzo Terreno

*Graphical Abstracts (for review)

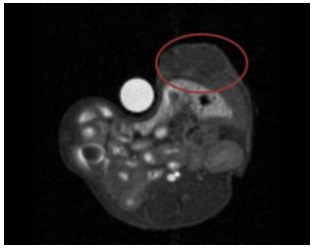

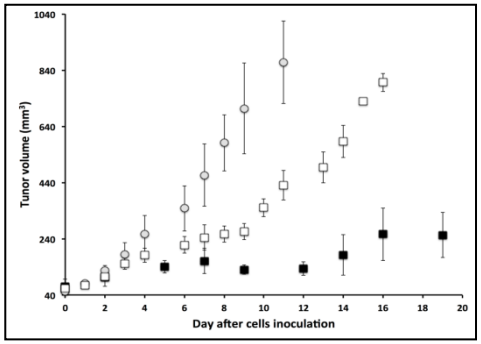

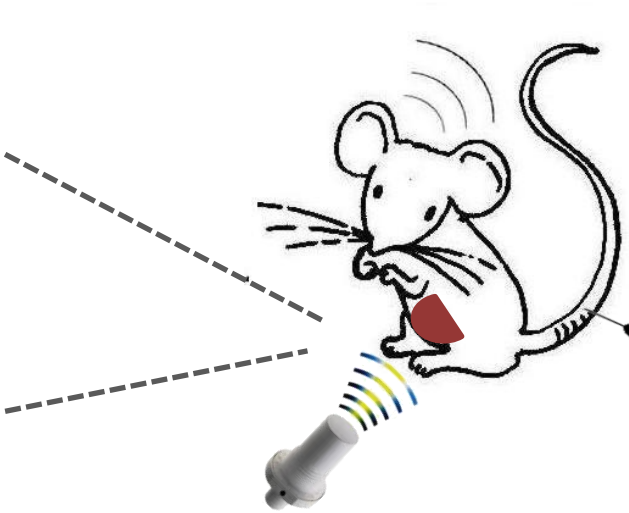

P-LINFU

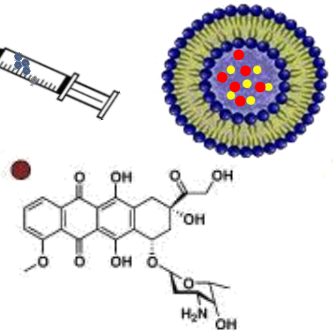

Doxorubicin

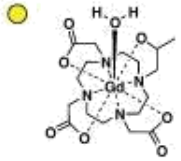

[Gd(HPDO3A)(H_2O)]

Preclinical *in vivo* MRI-guided visualization of Doxorubicin release from liposomes stimulated by pulsed low intensity non-focused Ultrasound

S. Rizzitelli[a], P. Giustetto[a,b], J.C.Cutrin[a], D. Delli Castelli[a], C. Boffa[a], M. Ruzza[a], V. Menchise[c], F. Molinari[d], S. Aime[a,b], E. Terreno[a,b,*]

[a] Center for Molecular Imaging, Department of Molecular Biotechnology and Health Sciences, University of Torino, Via Nizza 52, 10126 – Torino, Italy.

[b] Center for Preclinical Imaging, Department of Molecular Biotechnology and Health Sciences, University of Torino, Via Ribes 5, 10010 – Colleretto Giacosa (TO), Italy.

[c] Institute for Biostructures and Bioimages (CNR) c/o Molecular Biotechnology Center, University of Torino, Italy

[d] Biolab, Department of Electronics and Telecommunications, Politecnico di Torino, Torino, Italy

Abstract

The theranostic properties of a liposome containing Gadoteridol as MRI reporter and Doxorubicin have been assessed. The release of the drug and the contrast agent is triggered by the application of pulsed Low Intensity Non Focused Ultrasound (pLINFU). The theranostic system has been first characterized *in vitro*. Then, it has been tested *in vivo* on a syngeneic murine model of TS/A breast cancer. MRI offered an excellent guidance for monitoring the pLINFU-stimulated release of the drug by providing: i) an *in vivo* proof of the effective release of the liposomal content, and ii) an assessment of the therapeutic benefits of the overall protocol. *Ex vivo* fluorescence microscopy indicated that the good therapeutic outcome was originated from an improved diffusion of the drug in the tumor following the pLINFU stimulus. It has been found that the good diffusion of the drug in the tumor stroma is associated with the extravasation/accumulation of the liposomes in the tumor region. The theranostic agent herein developed has a high clinical translatability because the used liposomes, Doxorubicin, and MRI agent are entities already approved for human use.

1. Introduction

Currently, the design of theranostic procedures are under intense scrutiny to improve the efficiency of a pharmacological therapy and to optimize the therapeutic planning on an individual base (personalized medicine). Much attention is devoted to the development of systems that generate an imaging response as a function of the delivered and/or released drug. [1-3] In principle, imaging protocols for the visualization of drug delivery can be designed for most of the available imaging modalities (nuclear, CT, optical, US, MRI, and hybrid technologies).[4-6] However, when the imaging probe has to act as reporter of the release of a drug from a carrier, some techniques perform better in virtue of their peculiar characteristics in their contrast generation that makes possible to modulate the imaging response as a function of even subtle changes in the local microenvironment in which the reporting agent is distributed. Among them, MRI appears the candidate of choice because of the excellent spatio-temporal resolution, the possibility to reach deep tissues/organs without any limitations, and the rich portfolio of agents and contrast modalities available. [7] The motivation of using nanocarriers in the pharmacological field is mainly driven by the necessity of improving the therapeutic index of a drug. The rational is to influence the biodistribution of the drug to favor (by passive or active targeting) the accumulation and availability at the target organ, thereby improving therapeutic efficacy and reducing side effects. [8-9] For the nanomedicines currently approved for clinical use, the release of the drug occurs spontaneously, *i.e.* following the natural degradability of the nanocarrier interacting with tissue components.

However, it is expected that a significantly better control of the release can be achieved through a specific stimulation. Typically, triggering factors can be endogenous (chemical) or externally-applied (physical). [10-16]

The former approach relies on the design of nanocarriers whose releasing properties are modulated by the microenvironment of the diseased region (*e.g.* pH or overexpression of enzymes). Alternatively, physical stimuli can be locally and selectively applied to the lesion, thereby allowing a better spatio-temporal control of the release. Among the physical stimuli, heat is certainly the most commonly used. In addition to trigger the drug release, a local heating may be itself cytotoxic (e.g. hyperthermia and thermal ablation therapies) [17-19], thus synergically boosting the effect of the drug. Furthermore, it has been reported that a temperature rise can favor the extravascular accumulation of the drug due to an increase of the vascular permeability.[8] A local heating can be obtained by applying different kinds of external stimulation including high intensity focused US (HIFU), radiofrequency, alternating magnetic fields, and microwaves. [20-25]

To be responsive, the nanocarrier system has to be designed to release the drug in a narrow range of temperature, and nanotechnology offers different class of carriers with this property (*e.g.* liposomes, polymeric vesicles, micelles,…).[10-12, 21, 24, 26-33]

One of these systems, a temperature-sensitive liposomal formulation loaded with the anticancer drug doxorubicin, is currently in advanced clinical phase of development with the brand name of Thermodox® [34-35]. Concerning theranostics, a MRI-detectable version of this chemotherapeutic has been already developed and tested at preclinical level [36].

Importantly, when the stimulus is applied few minutes after the i.v. administration of the nanomedicine, the blood concentration of the chemotherapeutic is maximum, thus allowing the release, and the subsequent extravasation in the tumor, of a high amount of drug. Moreover, when the released drug is a small molecule (like doxorubicin) it can easily diffuse into the tumor, thus overcoming the high interstitial pressure that usually characterizes the solid lesions and limits the diffusion of the larger nanocarrier to few cell layers beyond the vessels. [6, 8, 37]

As alternative to heat, it has been recently demonstrated that drug release from liposomes can be also stimulated by using pulsed low intensity non focused US (pLINFU) [38-40].

pLINFU may be defined as pulsed, and non focused acoustic waves with intensity lower than 10 W/cm^2 and US frequencies from low (20 kHz) to therapeutic (1-3 MHz) range. Hence, differently from HIFU, the low energy associated with pLINFU cannot deliver enough energy to raise the temperature, and the release mechanism may primarily occur through mechanical interactions between the acoustic waves and the nanocarrier. In principle, pLINFU may offer some advantages over heating including: i) the extension of the triggered release to non temperature-sensitive

carriers, ii) the reduction of possible toxic side effects associated with the local heating, and iii) the unnecessary control of the local temperature.

Drug release from nanocarriers upon pLINFU exposure has been demonstrated *in vitro* in several literature reports. [30-37] Furthermore, the therapeutic benefit of this approach has been pre-clinically validated on tumor murine models.[40-42]

MRI has been widely used to guide the delivery of nanomedicines, mostly through the incorporation of contrast agents at the surface of the carrier (e.g. the bilayered shell in case of nanovesicles).[1] However, if the task is the MRI visualization of the release from nanovesicles, the best approach is certainly represented by the encapsulation of a hydrophilic paramagnetic agent in the aqueous nanovesicle core.[43-44] In fact, the use of "MRI quenched" carriers allows the detection of a contrast enhancement when the agent (and ideally the co-encapsulated drug) is released. [45-47]

We have recently demonstrated that MRI can be successfully used to guide the in vivo release of the clinically approved agent Gadoteridol upon the application of pLINFU stimuli. [48]

In the present study, this approach has been implemented to test a theranostic protocol in an experimental model of murine breast cancer, where MRI is used for both guiding the pLINFU-stimulated release of the anticancer drug Doxorubicin and monitoring the associated therapeutic outcome.

2. Materials and Methods

2.1 Chemicals

1,2-Dipalmitoyl-sn-glycero-3-phosphocoline (DPPC), 1,2-Distearoyl-sn-glycero-3-phosphocoline (DSPC), 1,2 Distearoyl-sn-glycero-3-phosphoethanolamine-N-[methoxy(polyethyleneglycol)-2000]Ammonium salt (DSPE-PEG2000), and Cholesterol were purchased from Avanti Polar Inc. (Alabaster, AL, USA). Doxorubicin hydrochloride was purchased from Sigma-Aldrich (St Louise, MO, USA). Gadoteridol [Gd(HPDO3A)(H_2O)] was kindly provided by Bracco Imaging SpA (Colleretto Giacosa (TO), Italy). The culture medium RPMI 1640, the biological buffers, foetal bovine serum (FBS), glutamine, penicillin-streptomycin mixture, and trypsin were purchased from Cambrex (East Rutherford, NJ, USA).

2.2 Liposomes preparation

Theranostic liposomes (herein named Gado-Doxo-Lipo) were prepared using the method based on the hydration of a thin lipid film. Briefly, the lipid components (DPPC/DSPC/Chol/DSPE-PEG2000

at molar ratio 10:5:4:1) were dissolved in chloroform (40 mg lipid/mL). The organic solvent was removed in vacuum until a thin film was formed. Then, the film was hydrated at 55°C with a solution of Gadoteridol 300 mM in $(NH_4)_2SO_4$ buffer 120 mM at pH 5.5. The suspension was progressively extruded at 55°C through polycarbonate filters of decreasing pore size: 4000 nm (two times), 200 nm (two times) and 100 nm (two times). Non encapsulated Gadoteridol was removed by exhaustive dialysis (two cycles 5 hours each, 4 °C) performed against isotonic HEPES buffer (pH 7.4). Next, paramagnetic liposomes were incubated overnight (at 34°C) with a 1mg/mL solution of Doxorubicin, stirring continuously the suspension. Finally, the non-encapsulated Doxorubicin was removed with two additional dialysis cycles (5 hours plus overnight) in HEPES buffer (pH 7.4, at 4°C). Dialysis was carried out in the dark.

Additional liposomal formulations (with the same membrane composition) were prepared, containing only Gadoteridol (Gado-Lipo), only Doxorubicin (Doxo-Lipo) or none of the theranostic companions (Control-Lipo).

2.3 Liposomes characterization

The mean hydrodynamic diameter of liposomes was determined using dynamic light scattering measurements (Malvern ZS Nanosizer, Malvern Instrumentation, UK) at 25°C and a scattering angle of 90°. 10 µL of liposomes suspension was diluted in 1 mL of filtered isotonic HEPES buffer (pH 7.4). Triplicate measurements were performed.

Liposomes prepared according to the procedure described above displayed a hydrodynamic diameter of 150 nm (PDI ≤ 0.1)

Gd(III) concentration (corresponding to the amount of Gadoteridol) was determined relaxometrically at 0.5 T (Stelar Spimaster, Mede (PV), Italy) measuring the longitudinal water protons relaxation rate (R_1) of the suspension after disruption of liposomes with Triton X-100 1 % v/v followed by the addition of concentrated hydrochloric acid and concomitant overnight heating at 180°C. [49] Doxorubicin concentration was determined fluorimetrically (λ_{ex} = 488 nm, λ_{em} = 590 nm, Fluoromax-4 spectrofluorimeter (Horiba Jobin Yvon)) after complete degradation of liposomes with the surfactant Triton X-100 1 % v/v. Typically, the concentration of Gadoteridol in the liposomes suspension was around 20 mM, while Doxorubicin concentration was around 1.8 mM (ca. 1 mg/mL). Thus, the molar ratio between encapsulated Gadoteridol and Doxorubicin was about 11:1.

2.4 Liposome stability

Liposomes stability was investigated by monitoring size, and Doxorubicin/ Gadoteridol release over time. Liposomes were stirred at 25°C and 37°C in isotonic HEPES buffer (pH 7.4). Size was measured for five consecutive days, then each 2 days for the next 15 days. Fluorescence and relaxometric measurements were performed daily.

2.5 US apparatus

Mice tumors were insonated with a 3.0 ± 0.1 MHz ultrasound transducer (designed and realized in collaboration with TEMAT s.r.l. - Torino). Piezoelectric ceramic flat disc (diameter 25 mm) transducer (STEMiNC Steiner & Martins, Inc – USA) was connected to a specific oscillator driving circuit. The circuit system used to generate the ultrasound energy in all the experiments included a tension generator (TTi EX354 RD- dual power supply 280 W), and a waveform generator (LXI KEITHLEY 3390 – 50 MHz) (Figure 1). The performance of the US transducer was controlled using an oscilloscope voltage signal (Tektronix TDS1001B) with an attenuated (100x) oscilloscope probe for the connection to the circuit, and multimeter (Fluke 87 V) for the current drawn. The multimeter was inserted in series between the power generator and the oscillating circuit to monitor current absorption from operating piezoelectric component and oscilloscope (TEKTRONIX TDS 1001 B – two channel – 40 MHz 500 MS/s) at oscillatory output point to evaluated sinusoidal voltage amplitude. The piezoelectric disk was housed and fixed inside a cylinder (metal alloy ultrasound transmitter) made by two round concentric chambers. The disc was cooled down with water circulating in the external chamber. The cooling system was turned on during all the insonation time.

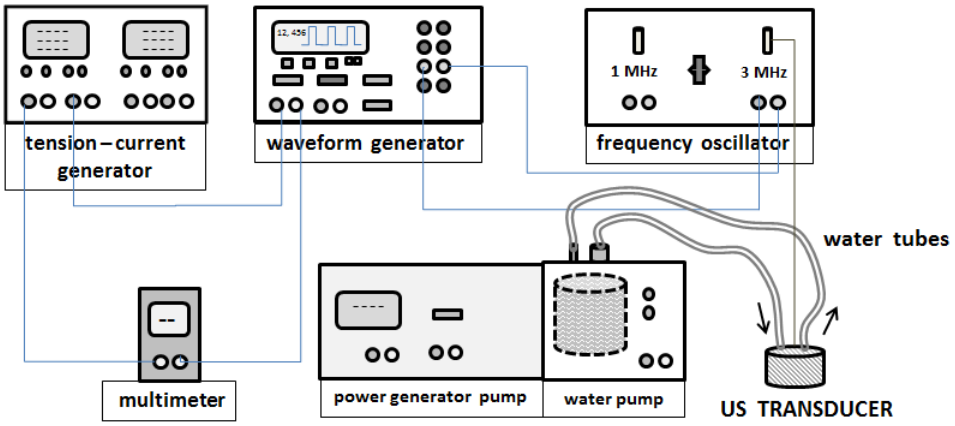

Figure 1. Scheme of the circuit used for the generation of pLINFU

2.6 Experimental pLINFU setup in vitro and in vivo

The experimental insonation setup used *in vitro* is illustrated in Figure 2.

The US transducer was placed in a plastic water-filled cylindrical box. The internal wall of the box was coated with an acoustic absorber sponge. The water level reached the transducer surface, so it can stabilize the temperature during the insonation time. A three-layers gel (ultrasonic gel + agar 10 % + ultrasonic gel) was used as interface between the transduced and the sample.

200 μL of the liposomal sample were put in a polyethylene terephthalate container.

The temperature of the sample was monitored during insonation and resulted to be unvaried at 19.6 ± 0.3 °C.

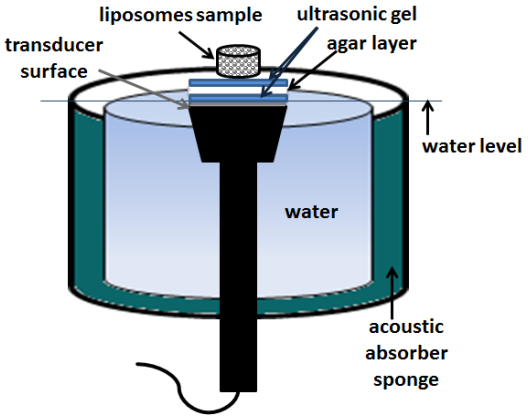

Figure 2. Insonation setup for *in vitro* experiments.

For *in vivo* experiments a dedicated 3 MHz transducer was used (acoustic intensity I = 3.3 ± 0.3 W/cm^2 and acoustic pressure P = 0.24 MPa). The tumor region was not immersed in water during pLINFU exposure. A multilayer interface composed of materials with decreasing values of acoustic impedance from tumor to transducer was designed (Figure 3) to minimize backscattering effects, thus optimizing the acoustic intensity efficiency of pLINFU hitting the lesion.

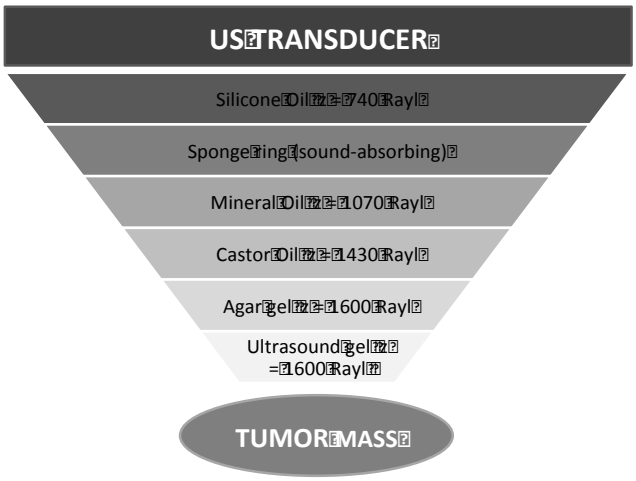

Figure 3. Composition of the multilayer interface used for *in vivo* experiments

2.7 Cells

TS/A cell line, derived from a spontaneous mammary adenocarcinoma which arose in a retired breeder BALB/c female,[50] were cultured as monolayer at 37°C in a 5% CO_2-containing humidified atmosphere. The culture medium was composed by RPMI 1640 supplemented with 10% (v/v) heat-inactivated FBS, 100 IU/mL penicillin, and 100 IU/mL streptomycin.

2.8 Animal model

Female BALB/c mice 6 weeks-old were purchased by Charles River Laboratories and kept in standard housing (12 h light-dark cycles) with a standard rodent chow and water available *ad libitum*. Experiments were performed according to the national regulations and were approved by the local animal experiments ethical committee. To induce mammary adenocarcinomas, 6×10^5 TS/A cells were inoculated subcutaneously in the mice abdomen. The experimental protocol (schematized in Figure 4) started one week after the cells inoculation, when the tumor reached a volume of 40-60 mm^3. Tumor volume was determined by MRI (multislice T_{2w} images). Mice were anesthetized by intramuscular injection of tielamine/zolazepam (Zoletil®) 20 mg/kg bw and xylazine (Rompum®) 5 mg/kg bw.

2.9 Release experiments in vitro

Liposomes were exposed to pLINFU with different characteristics (insonation time, pulse repetition frequency (PRF)) keeping the duty cycle to 50 %. After US stimulation, the sample was collected and both longitudinal water protons relaxation rate (R_1^{US}) and fluorescence were measured.
The release of Gadoteridol was determined using the following relationship:

$$Gadoteridol\ Release\ \% = \frac{R_1^{US} - R_1^{no-US}}{R_1^{Triton} - R_1^{no-US}} \cdot 100$$

where R_1^{Triton} refers to the relaxation rate measured for the sample in which Gadoteridol was fully released upon the addition of Triton X-100 1% v/v, and $R_1^{no\text{-}US}$ is the measurement of the sample not exposed to pLINFU.
The release of Doxorubicin was determined using an analogous equation:

$$Doxorubicin\ Release\ \% = \frac{F^{US} - F^{no-US}}{F^{Triton} - F^{no-US}} \cdot 100$$

where F^i is the fluorescence intensity of the sample.

2.10 Experimental planning

Mice enrolled in the main study were divided in three groups (n = 3 each):

- US-Group: mice injected with Gado-Doxo-Lipo (5 mg/kg bw of Doxorubicin, and 0.1 mmol/kg bw of Gadoteridol) and subjected to pLINFU exposure;
- NoUS-Group: mice injected with Gado-Doxo-Lipo (5 mg/kg bw of Doxorubicin, and 0.1 mmol/kg bw of Gadoteridol), but not subjected to pLINFU exposure
- Control Group: mice did not receive any treatment.

Animals were anesthetized 15 min before treatment. Before each MRI session, animals were weighed and the body temperature was acquired to prevent and monitor possible changes due to side effects of the drug.

MR images were acquired on a Bruker Avance 300 equipped with Micro 2.5 microimaging probe before Gado-Doxo-Lipo injection (PRE contrast image), and repeatedly from 10 min to 90 min after liposomes injection (for the US-group, pLINFU exposure was carried out immediately after liposomes injection). This image acquisition scheme was replicated at week 2 and 3.

Gado-Doxo-Lipo formulations were administered as bolus once a week for three weeks by injection in the tail vein.

A single pLINFU shot (3 MHz, total insonation time 2 min, duty cycle 50%, PRF 4 Hz, 37 V, was applied to the tumor region of US-group only.

The applied protocol is summarized in Figure 4.

Each MRI session included the acquisition of: i) a morphologic T_{2w} image (RARE sequence, TR 2000 ms, TE 3.4 ms, effective TE 27.20 ms, 4 averages, acquisition time 1.04 min, matrix size 128x128, slice thickness 1 mm, FOV 3x3 cm), ii) a series of T_{1w} images (Multi Slice Multi Echo sequence, TR 250 ms, TE 3.2 ms, 6 averages, acquisitions time 3.12 min, matrix size 128x128, slice thickness 1 mm, FOV 3x3 cm).

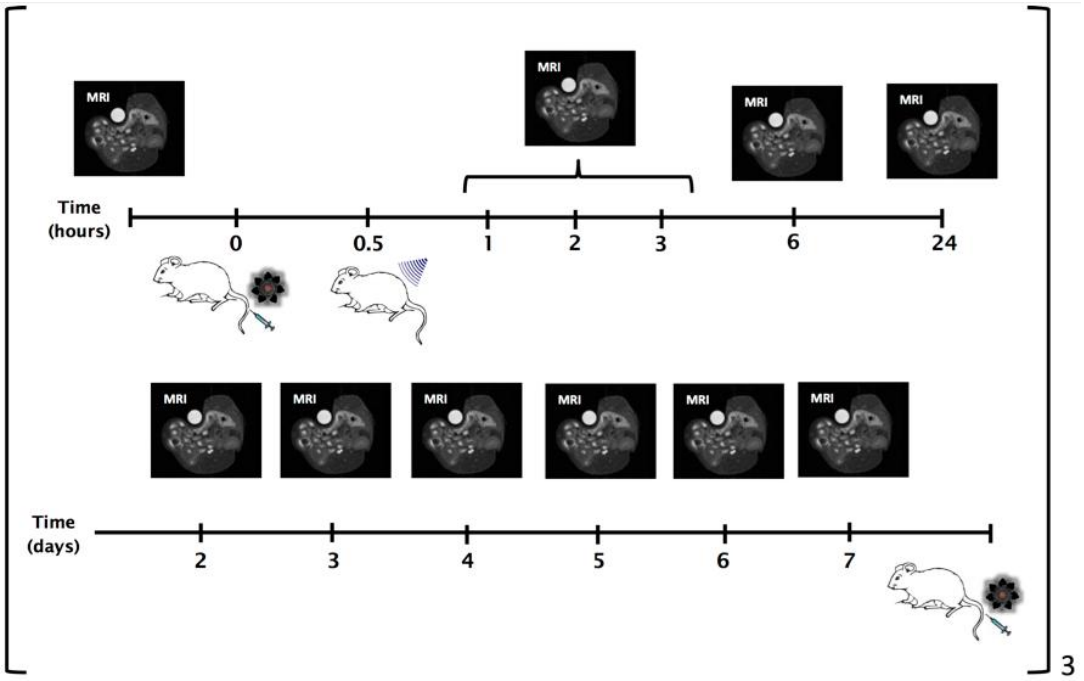

Figure 4. Schematic view of the experimental planning

T_{2w} images served to define the morphology and draw the ROI (Region of Interest) on the organs of interest (tumor, liver, spleen, kidneys, bladder). ROIs were then transposed on T_{1w} images (acquired with the same geometry), and the T_1 Contrast-to-Noise Ratio (CNR(T_1)) was measured as follows:

$$CNR(T_1) = \frac{SI_{(A)} - SI_{(B)}}{SDV_{(B)}}$$

where $SI_{(A)}$ is the MRI signal intensity of a given ROI, $SI_{(B)}$ is the signal from the and $SDV_{(B)}$ is the standard deviation of the signal noise.[51-53]

Values reported in the graphs are expressed as CNR(T_1)%, which correlates CNR(T_1) POST-contrast to the corresponding PRE-contrast value.

2.11 Histological evaluations

Mice were sacrificed by cervical dislocation at different times (immediately after pLINFU application (t=0), then 6 h and 24 h after liposomes injection). Tumors were gently removed, embedded in OCT, flash frozen in liquid nitrogen, and then stored at -80°C until further processing. 5 µm cryosections, obtained at different depth levels of the tumor, were cut, fixed in acetone 100% for 10 minutes at room temperature, and preserved in the dark at 4°C. The sections were stained with hematoxylin and eosin using a standard protocol for histological assessment of cellular density and necrosis under a light microscope (10x and 20x magnification).

2.12 Laser Scanning Confocal Microscopy (LSCM)

Frozen tumor microsections (obtained as reported above) were analyzed with Laser Scanning Confocal Microscopy (Leica TCS SP5, Leica Microsystem Srl.). Experiments were carried out using a 20x dry lens and a 63x oil-wet lens. Doxorubicin was visualized in the red channel (λ_{ex} 488 nm; λ_{em} 590 nm). Hoescht dye (Sigma-Aldrich) was added for nuclear staining and visualized in the blue channel (λ_{ex} 358 nm; λ_{em} 461 nm).

2.13 Texture analysis of the LSCM images

Texture analysis aims at numerically evaluating the smoothness, coarseness, and regularity of the pixel distribution in an image. Among all the texture descriptors that have been proposed [54], we chose the following two: Haralick's Entropy (I_{Entr}) and Haralick's Homogeneity (I_{hmg}) [55]. The Haralick features (also called second order statistical descriptors) are based on the Gray Level Co-occurrence Matrix (GLCM). Let the image be represented by a $M \times N$ gray-scale matrix $I(i, j)$, where each element of the matrix indicates the intensity of a single pixel in the image. The co-occurrence matrix $C(i,j \mid \Delta x, \Delta y)$ is the second-order probability function estimation that denotes the rate of occurrence of a pixel pair with gray levels i and j, given the distances between the pixels are Δx and Δy in the x and y directions, respectively. The co-occurrence matrix $C(i, j \mid \Delta x, \Delta y)$ can be written as

$$C(i,j \mid \Delta x, \Delta y) = \left| \left\{ (p,q), (p+\Delta x, q+\Delta y) : I(p,q) = i, I(p+\Delta x, q+\Delta y) = j \right\} \right|$$

where $(p,q)(p+\Delta x, q+\Delta y) \in MxN$, $d = (\Delta x, \Delta y)$, and $|\cdot|$ denotes the cardinality of a set. The probability that a gray level pixel i is at a distance $(\Delta x, \Delta y)$ away from the gray level pixel j is given by

$$P(i,j) = \frac{C(i,j)}{\sum C(i,j)}$$

The homogeneity I_{hmg} can be defined as:

$$I_{hmg} = \sum_{i=0}^{N-1} \sum_{j=0}^{N-1} \frac{1}{1+(i-j)^2} P(i,j)$$

and the entropy I_{Entr} as:

$$I_{Entr} = -\sum_{i=0}^{N-1}\sum_{j=0}^{N-1} P(i,j)\log(P(i,j))$$

When the image is composed or large regions having same intensity, the probability *P(i,j)* grows, because there are locally a lot of occurrence of pixels with same intensity is all directions. Conversely, when the image has diffused and widespread intensities *P(i,j)* decreases. Hence, I_{hmg} is expected to decrease as the color in the image is more and more diffused, whereas I_{Entr} is expected to increase. Homogeneity is bound between 0 and 1, whereas entropy has a lower bound to 0 but it is not upper-bounded.

Usually, texture analysis is used to classify the morphological features of an image. We applied texture analysis to the layer colors of the histological images, with the objective of quantifying the spatial organization of the Doxorubicin. Hence, we first decomposed the color images acquired by confocal microscopy into the red, blue and, background channels by using the Ruifrock's decomposition [56]; then we applied the texture analysis to the red channel (indicative of the Doxorubicin localization).

3. Results

3.1 In vitro release

The pLINFU-stimulated release of the theranostic companions (Doxorubicin and Gadoteridol) from stealth liposomes was first tested *in vitro*. The percentage of release was determined as a function of PRF keeping constant the duty cycle (50%). The temperature of the sample was constantly monitored and never exceeded 19.6°C, *i.e.* well below the gel-to-liquid phase transition temperature of the liposome bilayer (*ca.* 41°C), thereby indicating that the release was not heat-mediated.

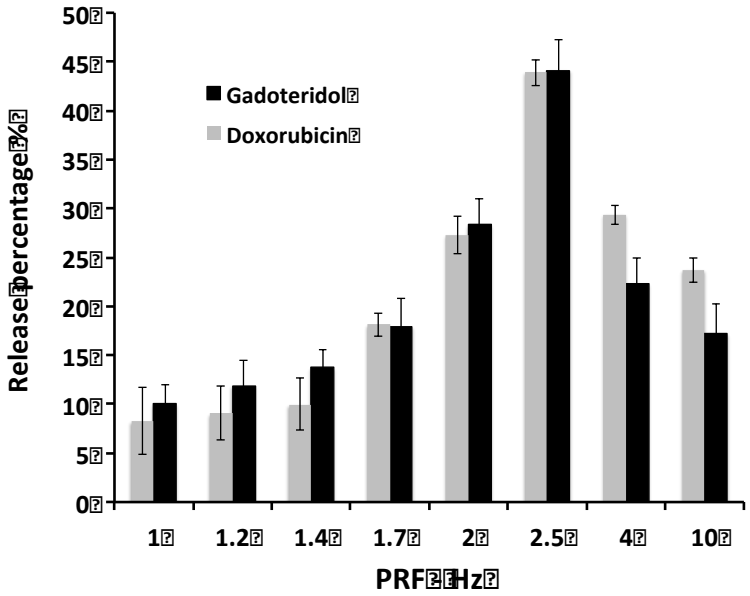

Figure 5. pLINFU-stimulated release of Doxorubicin and Gadoteridol from stealth liposomes *in vitro*. The release was evaluated by spectrofluorimetry (Doxorubicin) and relaxometry (Gadoteridol), respectively. Liposomes were insonated by non-focused US, total time 2 min, duty cycle 50%.

After stimulation, each sample was collected and the release of Gadoteridol and Doxorubicin was determined by relaxometry and spectrofluorimetry, respectively.
The results confirmed the strong dependence of the release on PRF values, and, very important, highlighted the equivalent release of the two compounds over the entire PRF range investigated (Fig. 5). The maximum observed release *in vitro* (about 45 %) was measured at the PRF value of 2.5 Hz.
This finding gave a strong support to the possibility of using MRI as *in vivo* guidance to reliably report the effective intratumour release of the drug after local pLINFU application.

3.2 Imaging release in vivo by MRI

Three mice groups (n=3) were enrolled in the *in vivo* study, but only two of them (US- and NoUS-groups) were injected with the theranostic liposomes (Gado-Doxo-Lipo).
The US-group was insonated immediately after the liposomes injection to maximize the amount of the released drug, and, in parallel, to increase the associated MRI contrast.
Mice of both groups were subjected to MRI. T_1 contrast to noise ratio (CNR(T_1)) was consecutively measured in tumour, liver, spleen, kidneys and bladder in the first 90 minutes after the liposomes injection. MR images were then acquired after 6 hours, and daily for 7 days. This experimental scheme was replicated for three weeks (Fig. 4).
Figure 6 reports the CNR(T_1) values (expressed as percentage) measured in the tumour of US- and NoUS-groups.

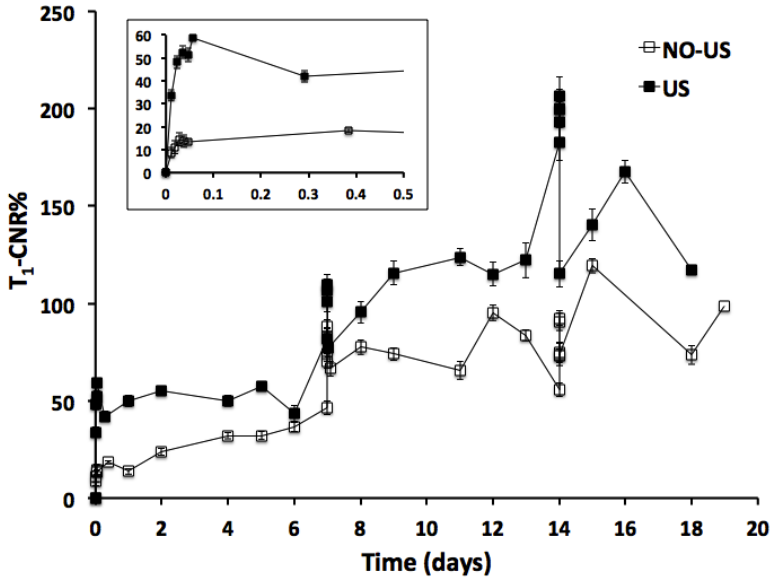

Figure 6. Time evolution of CNR(T_1)% measured in the tumour for US- and NoUS mice groups after injection of Gado-Doxo-Lipo. Liposomes were injected IV at days 0, 7 and 14 with a dose of 0.1 mmol/kg bw of Gadoteridol and 5 mg/kg bw of Doxorubicin. The inset shows the evolution after the first injection.

pLINFU-stimulated mice showed significantly higher CNR(T_1) values than untreated group to release of Gadoteridol. The enhancement for the US-group was maximal immediately after the stimulation and decreased within the successive 6 hours. Conversely, a much smaller enhancement was detected in NoUs-Group, immediately after the injection, likely as a consequence of the intratumour circulation of the intact "MRI-quenched" liposomes. A representative example of the MR images acquired after liposomes injection is reported in the Supplementary Material (Fig. S1). Very interestingly, after the initial decrease, CNR(T_1) values slowly steadily recovered from day 1 to days 3/4. Likely, this long-term enhancement, which was also observed for the NoUS-group, could be the consequence of the degradation of the paramagnetic liposomes internalized by tumour stroma cells (mainly cancer cells and macrophages) as already observed after the intratumour injection of Gadoteridol-loaded liposomes. [57]

To support this hypothesis, a group of mice (n = 3) were injected with free Gadoteridol (that cannot be taken up by stromal cells) in presence of Doxo-Lipo. The CNR(T_1)% values in the tumour were measured until 4 days after administration (no pLINFU). The T_1 contrast enhancement observed (Fig. S2) was similar to the US-group for the first 6 hours, but, then, instead of increasing, the contrast stabilized to the basal pre-injection value.

As Gadoteridol has a predominant renal excretion (blood half-lifetime of *ca.* 3 hours in mice[48]), it is expected that the pLINFU-triggered release of the agent in the tumour is associated with the accumulation in kidneys calix and bladder. The presence of a very bright T_1 contrast in the latter

compartment (Fig. 7) after the tumor insonation was taken as a clear evidence of the effective intratumour release of the MRI probe triggered by the local pLINFU application.

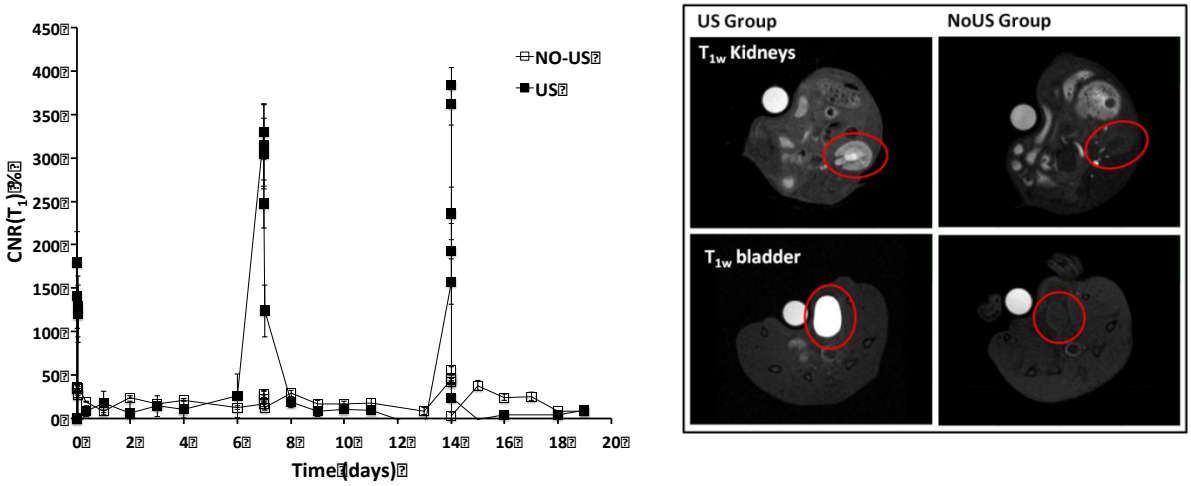

Figure 7. Left: temporal evolution of CNR(T_1) values measured calyx of the kidneys for US- and NoUS-groups. Right: T_{1w} MR images of kidneys (top row) and bladder (bottom row) 15 minutes after liposomes injection.

A further indirect confirmation of the intratumour release of Gadoteridol in the US-group was gained by measuring the contrast in liver and spleen where it is well known liposomes rapidly accumulated after injection. The data reported in Figures S3 and S4 indicates that the CNR(T_1) values measured in these organs were higher for NoUS-group than US-treated group. Most likely, this observation can be interpreted considering that the pLINFU exposure reduced the amount of paramagnetic liposomes circulating in the blood, thereby decreasing the liver and spleen uptake of the liposomes, with the consequent diminution of T_1 contrast.

3.3 *Ex-vivo confocal microscopy*

To support the results obtained *in vivo* by MRI, a confocal fluorescence microscopy study was carried out on tumour sections of US- and No-US-groups explanted at different times (0, 6 and 24 hours) post-injection of Gado-Doxo-Lipo. Tumors excised immediately after the pLINFU stimulation showed a diffuse fluorescence (Fig. 8 left), thereby indicating a quite homogeneous distribution of the drug into the lesion. Conversely, images from NoUS-group (Fig. 8 right) displayed a much more focused fluorescence, which was not detected in the necrotic areas. To obtain a quantitative analysis of the confocal images that could numerically assess the different distribution of the fluorescent signal in the tissue, a texture analysis approach described in section

2.13 was applied. The results are reported in Table S1 and confirmed the different distribution of the signal between US- and NoUS-groups. The homogeneity of the image was equal to 0.56 for the NoUS-image (Fig. 8 right) and to 0.46 for the US (Fig. 8 left). The entropy increased from 5.13 (NoUS) to 6.53 (US), thus documenting the more diffused distribution of the Doxorubicin after pLINFU insonation.

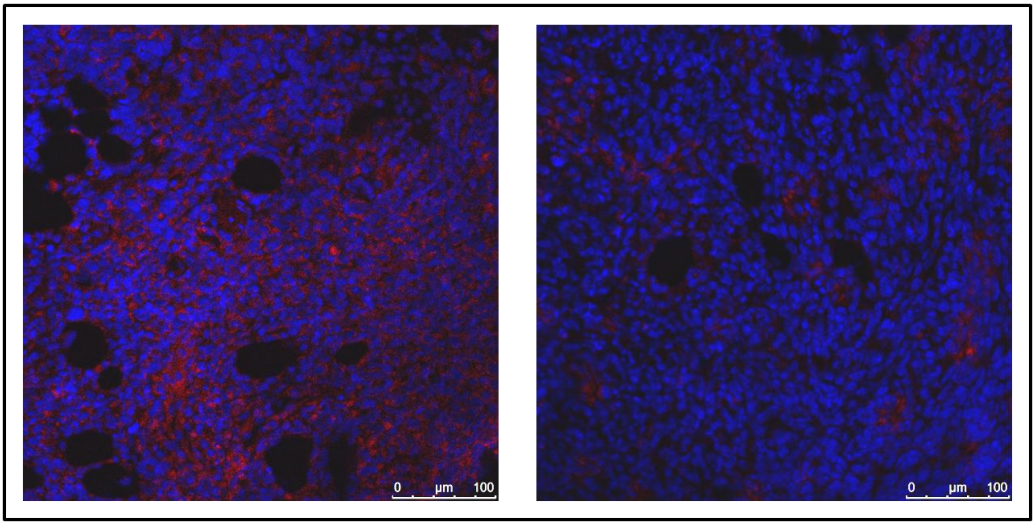

Figure 8. CLSM images of tumour sections from US- (left) and NoUS (right) groups explanted just after Gado-Doxo-Lipo injection. (100x, DAPI staining).

3.3 Insights on the release mechanism in vivo

To better understand the mechanism underlying the pLINFU-mediated extravascular diffusion of Doxorubicin in the tumour, additional experiments were carried out upon injection of the free drug with or without pLINFU exposure.

Quite surprisingly, in both cases fluorescence microscopy indicated a clear intravascular distribution of the drug (Fig. 9, left and middle), thus suggesting that the insonation alone did not affect the permeability of the tumour vasculature.

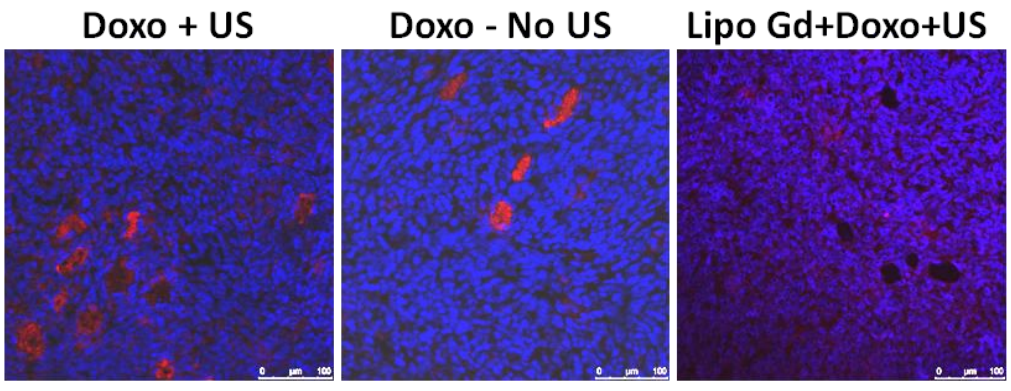

Figure 9. CLSM images of tumour sections of mice injected with free Doxorubicin exposed (left) or not exposed (middle) to pLINFU. Right: tumour of a mouse injected with free Doxorubicin and Gadoteridol-loaded liposomes and exposed to pLINFU. Tumours were explanted just after drug administration (100x, DAPI staining).

However, if free Doxorubicin was co-injected with Gadoteridol-loaded liposomes, a clear intratumor diffusion of the drug (confirmed by texture analysis, see Table S1) was observed after pLINFU stimulus (Fig. 9, right). This finding highlighted the key role played by liposomes to allow the extravasation of the released drug, thus favouring the good diffusion in the tumour. The texture analysis confirmed the higher diffused pattern of the Doxorubicin: when Doxorubicin was co-injected with Gadoteriol-loaded liposomes and then insonated by pLINFU, the homogeneity was very low (0.25) and the entropy was high (8.75). When insonation was performed after injection of Doxorubicin alone, the homogeneity was 5.53 and the entropy was 0.50; when Doxorubicin was injected without any insonation, homogeneity was 2.16 and entropy was 0.82 (Table S1).
The effect of liposomes to mediate the permeabilization of the tumour endothelium was also demonstrated by comparing the T_1 contrast enhancement of pLINFU-exposed mice injected with free Gadoteridol with or without the co-presence of liposomes. The noticeable increase in the CNR(T_1) values observed in the presence of the carrier (Fig. 10) is a clear indication of the extravasation of the paramagnetic agent.

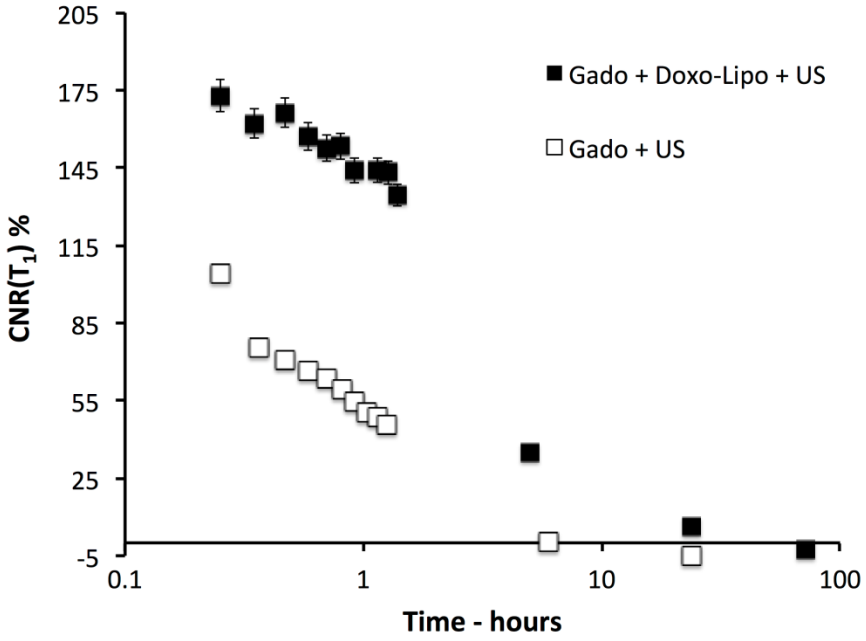

Figure 10: Temporal evolution of CNR(T_1) values measured in the tumor area for animals treated with free Gadoteridol in presence (filled square) or absence (open square) of liposomes, followed by pLINFU exposure.

3.4 Monitoring therapeutic efficacy by MRI

The acquisition of morphological T_{2w} MR images allowed the accurate monitoring of the tumour progression for US-, NoUS-, and Control groups (Fig. 11).

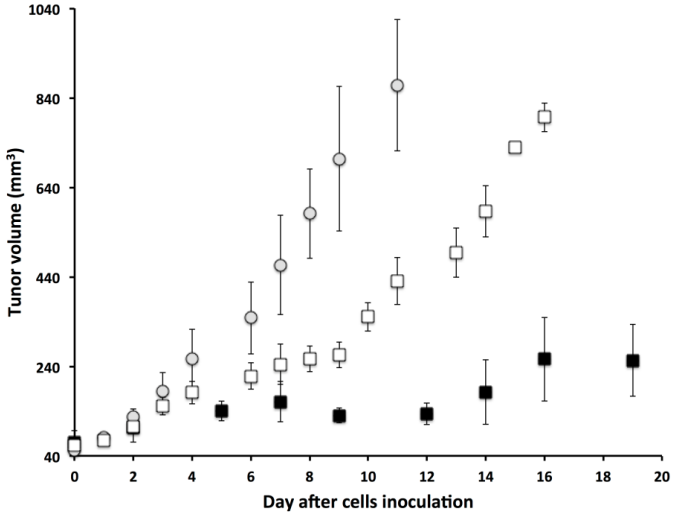

Figure 11: Tumour progression as a function of the time elapsed from the monitored by MRI for US-(filled square), NoUS (open square), and Control (grey filled circles) groups. Time zero corresponds to the moment in which the tumour volume was around 60 mm^3. Gado-Doxo-Liposomes were injected at days 0, 7, and 14. pLINFU stimulation (for US-group only) was carried out just after the injection.

The treatment with the theranostic formulation significantly delayed the tumour growth, and a tumor shrinkage of *ca.* 50 % (compared to Control) was observed after 10 days. Very important, the tumour exposure to pLINFU considerably improved the therapeutic outcome with an additional shrinkage (with respect to the NoUS-group) of *ca.* 60 % after 16 days of treatment.

4. Discussion

4.1 In vitro release

The use of MRI to visualize the release of Doxorubicin from liposomes relies on the design of a MRI agent that "lights up" in concomitance with the release of the drug. As reported by us and others, [20, 46, 48, 58] the encapsulation of a high amount of a hydrophilic paramagnetic Gd-complex in the aqueous cavity of liposomes yields a system whose T_1 relaxivity is markedly

"quenched". This effect is due to the slow diffusion of water molecules across the liposome bilayer. Consequently, when the agent is released from the carrier, the contrast switches on. As the MRI agent (here Gadoteridol) and the drug have different physico-chemical properties, it was of fundamental importance to prove that the pLINFU stimulation led to the co-release of both molecules. The data reported in Fig. 5 clearly indicate that the two compounds share an almost identical release profile as a function of the PRF value of the insonation, with a maximum release observed at 2.5 Hz.

Though quite unexpected (owing to the quite different physico-chemical properties of the two compounds), this finding is crucial for the use of Gadoteridol as imaging marker of the release of Doxorubicin. A similar result was reported for the same compounds encapsulated in thermosensitive liposomes and exposed to HIFU stimulus.[20] However, though the liposome formulation used in this work is expected to be temperature sensitive (DPPC has a gel-to-liquid transition temperature of *ca.* 41°C), the temperature of the insonated sample never exceeded 19.6°C, thereby confirming that the pLINFU-controlled release was not mediated by thermal effects.

4.2 In vivo experiments

The performance of the theranostic protocol herein proposed was tested *in vivo* on a syngeneic mouse model of breast cancer. The tumor was induced by the subcutaneous inoculation of TS/A cells. When the tumor reached a volume ranging from 50-70 mm^3 (around 1 week post inoculation), the animals were enrolled in the study.

Three experimental groups were planned, namely two treated with Lipo-Doxo-Gado (US and NoUS) and one control.

The timeline of the experimental imaging protocol is sketched in Figure 4 and summarized in Section 2.10.

To maximize the release of the drug in the diseased region, the pLINFU stimulus was applied locally at the tumor area using a suitably developed multilayer interface to preserve as much as possible the intensity of the transmitted waves from the transducer to tumor. Furthermore, it was deemed useful to apply the pLINFU stimulation few minutes after the liposomes injection, *i.e.* when the amount of liposomes at the tumor region is the highest one.

The data reported in Figure 6 indicate that the T_1 contrast measured in the tumors of the pLINFU-treated mice was higher than group that not received pLINFU, thus indicating the effective role of the US stimulation to generate the intratumor release of the agent from the carrier. Further support

to this view came by the strong MRI signal detected in kidneys and bladder for the treated mice only (Figure 7), as consequence of the fast renal excretion of free Gadoteridol.
Even the lower contrast observed in liver (Figure S3) and spleen (Figure S4) of the pLINFU exposed mice with respect to the US-untreated group is likely the result of the release of the paramagnetic agent in the tumor.
In virtue of its fluorescence properties, the intratumor diffusion of Doxorubicin could have been detected by confocal fluorescence microscopy on tissue sections of explanted tumors. Importantly, pLINFU-treated tumors displayed a much more intense and diffuse fluorescence than the US-untreated specimens (Figure 8). The higher entropy and lower homogeneity of the image corresponding to the pLINFU insonated group (Fig. 8 left) demonstrated a more diffused pattern of the Doxorubicin, that was numerically found to be more concentrated in the No-US image (Fig. 8 right).
To get more insight into the mechanism underlying the diffusion of the drug in the lesion, additional experiments were carried out.
Interestingly, when free Doxorubicin was injected, no drug was detected in the tumor stroma in confocal microscopy images, neither after pLINFU application. In both cases, the texture descriptors were indicative of a very concentrated pattern, with low entropy and high homogeneity (Fig. 9 left and middle). This observation strongly supports the view that liposomes have an active role to allow the intratumor diffusion of the drug released in the vasculature.
A further confirmation of the role of liposomes was gained *in vivo* by measuring the intratumor T_1 contrast after administrating free Gadoteridol with or without co-injection of Doxo-Lipo (Figure 10). The much higher MRI signal measured in the presence of liposomes is the consequence of the liposome/pLINFU-mediated extravasation of the MRI agent across the endothelium.
On this basis, it can be conjectured that liposomes act as a sort of acoustic resonator in presence of pLINFU. The waves generated by the interaction between US and liposomes can induce, like sonoporation, the permeabilization of the vascular endothelium.
Interestingly, we observed similar permeabilization effects *in vitro* applying pLINFU to a cell suspension added with liposomes.[59]
Looking at the time evolution of the T_1 contrast displayed in Figure 5, another interesting observation can be drawn. In both US- and NoUS-groups, after an initial decrease of the contrast due to the wash out of the released Gadoteridol and the decrease of the amount of circulating paramagnetic liposomes, the contrast in the tumor region was maintained and eventually increased reaching a maximum value after 4-5 days post-injection. This delayed contrast enhancement was comparable or even higher than the CNR(T_1) values measured just after the liposomes injection. As

tumor stroma cells do not internalize Gadoteridol, the long-term signal enhancement is likely associated with the cellular uptake of the paramagnetic liposomes. This hypothesis was supported by the lack of the delayed enhancement observed after the injection of free Gadoteridol (Figure S2). This finding is highly relevant for the clinical translation of the theranostic construct based on liposomes, and will deserve further studies that are beyond the scope of this work.

4.3 Therapeutic benefits

The therapeutic outcome of the herein proposed theranostic protocol was assessed by measuring (by morphological MRI) the change of the tumor volume for US-, NoUS-, and Control-groups.
The results reported in Figure 11 highlight the excellent performance of the pLINFU treatment that significantly delayed (starting from the second week of treatment) the tumor growth with respect to the US-untreated group.

Conclusions

This study demonstrated that MRI can successfully guide the intratumor release of Doxorubicin from liposomes stimulated by the local application of pLINFU. The method relies on the encapsulation of the clinically approved MRI agent Gadoteridol in liposomes already used in clinical chemotherapy.
This procedure may provide an efficient imaging tool to monitor the effective release of the drug *in vivo* on a personalized base. The investigated theranostic agent has a high clinical translatability. Finally, besides offering an excellent spatio-temporal guidance of the drug release process, pLINFU stimulation leads to a significant benefit in the therapeutic outcome of the proposed nanomedicine, when compared with the pharmacological results in the non-stimulated procedure. Furthermore, several improvements can be envisaged such as the design of systems with enhanced ability to generate MRI contrast, the increase of the release efficiency through the optimization of the pLINFU application scheme, and the search for methods to favor the extravasation and the diffusion of the drug in the tumor.

Bibliography

1. Terreno, E., F. Uggeri, and S. Aime, *Image guided therapy: The advent of theranostic agents.* Journal of Controlled Release, 2012. **161**(2): p. 328-337.
2. Prabhu, P. and V. Patravale, *The Upcoming Field of Theranostic Nanomedicine: An Overview.* Journal of Biomedical Nanotechnology, 2012. **8**(6): p. 859-882.
3. Sumer, B. and J.M. Gao, *Theranostic nanomedicine for cancer.* Nanomedicine, 2008. **3**(2): p. 137-140.
4. Weissleder, R. and M.J. Pittet, *Imaging in the era of molecular oncology.* Nature, 2008. **452**(7187): p. 580-589.
5. Massoud, T.F. and S.S. Gambhir, *Molecular imaging in living subjects: seeing fundamental biological processes in a new light.* Genes & Development, 2003. **17**(5): p. 545-580.
6. Weissleder, R., *Molecular imaging: Exploring the next frontier.* Radiology, 1999. **212**(3): p. 609-614.
7. Jacobs, R.E. and S.R. Cherry, *Complementary emerging techniques: high-resolution PET and MRI.* Current Opinion in Neurobiology, 2001. **11**(5): p. 621-629.
8. Manzoor, A.A., et al., *Overcoming Limitations in Nanoparticle Drug Delivery: Triggered, Intravascular Release to Improve Drug Penetration into Tumors.* Cancer research, 2012. **72**(21): p. 5566-5575.
9. Torchilin, V., *Liposomes in Drug Delivery*, in *Fundamentals and Applications of Controlled Release Drug Delivery*, J. Siepmann, R.A. Siegel, and M.J. Rathbone, Editors. 2012, Springer: New York. p. 289-328.
10. Ponce, A.M., et al., *Hyperthermia mediated liposomal drug delivery.* International Journal of Hyperthermia, 2006. **22**(3): p. 205-213.
11. Koning, G.A., et al., *Hyperthermia and Thermosensitive Liposomes for Improved Delivery of Chemotherapeutic Drugs to Solid Tumors.* Pharmaceutical Research, 2010. **27**(8): p. 1750-1754.
12. Needham, D., et al., *A new temperature-sensitive liposome for use with mild hyperthermia: Characterization and testing in a human tumor xenograft model.* Cancer research, 2000. **60**(5): p. 1197-1201.
13. Torres, E., et al., *Improved paramagnetic liposomes for MRI visualization of pH triggered release.* Journal of Controlled Release, 2011. **154**(2): p. 196-202.
14. Kuppusamy, P., et al., *Noninvasive imaging of tumor redox status and its modification by tissue glutathione levels.* Cancer research, 2002. **62**(1): p. 307-312.
15. Mellal, D. and A. Zumbuehl, *Exit-strategies - smart ways to release phospholipid vesicle cargo.* Journal of Materials Chemistry B, 2014. **2**(3): p. 247-252.
16. Zhu, L. and V.P. Torchilin, *Stimulus-responsive nanopreparations for tumor targeting.* Integrative Biology, 2013. **5**(1): p. 96-107.
17. Singh, R. and S.V. Torti, *Carbon nanotubes in hyperthermia therapy.* Advanced Drug Delivery Reviews, 2013. **65**(15): p. 2045-2060.
18. Bazrafshan, B., et al., *Temperature imaging of laser-induced thermotherapy (LITT) by MRI: evaluation of different sequences in phantom.* Lasers in Medical Science, 2014. **29**(1): p. 173-183.
19. Kostrzewa, M., et al., *Microwave Ablation of Osteoid Osteomas Using Dynamic MR Imaging for Early Treatment Assessment: Preliminary Experience.* Journal of Vascular and Interventional Radiology, 2014. **25**(1): p. 106-111.
20. de Smet, M., et al., *Magnetic Resonance Guided High-Intensity Focused Ultrasound Mediated Hyperthermia Improves the Intratumoral Distribution of Temperature-Sensitive Liposomal Doxorubicin.* Investigative Radiology, 2013. **48**(6): p. 395-405.
21. Grull, H. and S. Langereis, *Hyperthermia-triggered drug delivery from temperature-sensitive liposomes using MRI-guided high intensity focused ultrasound.* Journal of Controlled Release, 2012. **161**(2): p. 317-327.
22. Negussie, A.H., et al., *Formulation and characterisation of magnetic resonance imageable thermally sensitive liposomes for use with magnetic resonance-guided high intensity focused ultrasound.* International Journal of Hyperthermia, 2011. **27**(2): p. 140-155.
23. Ranjan, A., et al., *Image-guided drug delivery with magnetic resonance guided high intensity focused ultrasound and temperature sensitive liposomes in a rabbit Vx2 tumor model.* Journal of Controlled Release, 2012. **158**(3): p. 487-494.

24. Li, L., et al., *Mild hyperthermia triggered doxorubicin release from optimized stealth thermosensitive liposomes improves intratumoral drug delivery and efficacy.* Journal of Controlled Release, 2013. **168**(2): p. 142-150.
25. Lanza, G.M., et al., *Assessing the barriers to image-guided drug delivery.* Wiley Interdisciplinary Reviews-Nanomedicine and Nanobiotechnology, 2014. **6**(1): p. 1-14.
26. Fernando, R., et al., *MRI-Guided Monitoring of Thermal Dose and Targeted Drug Delivery for Cancer Therapy.* Pharmaceutical Research, 2013. **30**(11): p. 2709-2717.
27. Lanza, G.M., et al., *Assessing the barriers to image-guided drug delivery.* Wiley Interdisciplinary Reviews-Nanomedicine and Nanobiotechnology, 2014. **6**(1): p. 1-14.
28. Dewhirst, M.W., et al., *Novel Approaches to Treatment of Hepatocellular Carcinoma and Hepatic Metastases Using Thermal Ablation and Thermosensitive Liposomes.* Surgical Oncology Clinics of North America, 2013. **22**(3): p. 545-+.
29. McDaniel, J.R., M.W. Dewhirst, and A. Chilkoti, *Actively targeting solid tumours with thermoresponsive drug delivery systems that respond to mild hyperthermia.* International Journal of Hyperthermia, 2013. **29**(6): p. 501-510.
30. Sharma, D., T.P. Chelvi, and R. Ralhan, *Thermosensitive liposomal taxol formulation: heat-mediated targeted drug delivery in murine melanoma.* Melanoma Research, 1998. **8**(3): p. 240-244.
31. Papahadjopoulos, D., et al., *Phase transitions in phospholipid vesicles. Fluorescence polarization and permeability measurements concerning the effect of temperature and cholesterol.* Biochimica et biophysica acta, 1973. **311**(3): p. 330-48.
32. Dicheva, B.M. and G.A. Koning, *Targeted thermosensitive liposomes: an attractive novel approach for increased drug delivery to solid tumors.* Expert Opinion on Drug Delivery, 2014. **11**(1): p. 83-100.
33. Li, L., et al., *A novel two-step mild hyperthermia for advanced liposomal chemotherapy.* Journal of Controlled Release, 2014. **174**: p. 202-208.
34. May, J.P. and S.D. Li, *Hyperthermia-induced drug targeting.* Expert Opinion on Drug Delivery, 2013. **10**(4): p. 511-527.
35. Needham, D., et al., *Materials characterization of the low temperature sensitive liposome (LTSL): effects of the lipid composition (lysolipid and DSPE-PEG2000) on the thermal transition and release of doxorubicin.* Faraday Discussions, 2013. **161**: p. 515-534.
36. Langereis, S., et al., *Paramagnetic liposomes for molecular MRI and MRI-guided drug delivery.* Nmr in Biomedicine, 2013. **26**(7): p. 728-744.
37. Chen, X.Y., S.S. Gambhlr, and J. Cheon, *Theranostic Nanomedicine.* Accounts of Chemical Research, 2011. **44**(10): p. 841-841.
38. Lin, C.Y., et al., *Ultrasound sensitive eLiposomes containing doxorubicin for drug targeting therapy.* Nanomedicine-Nanotechnology Biology and Medicine, 2014. **10**(1): p. 67-76.
39. Lin, H.Y. and J.L. Thomas, *Factors affecting responsivity of unilamellar liposomes to 20 kHz ultrasound.* Langmuir, 2004. **20**(15): p. 6100-6106.
40. Evjen, T.J., et al., *In vivo monitoring of liposomal release in tumours following ultrasound stimulation.* European Journal of Pharmaceutics and Biopharmaceutics, 2013. **84**(3): p. 526-531.
41. Staples, B.J., et al., *Role of frequency and mechanical index in ultrasonic-enhanced chemotherapy in rats.* Cancer Chemotherapy and Pharmacology, 2009. **64**(3): p. 593-600.
42. Knodler, M., et al., *An analysis of toxicity in patients with recurrent and/or metastatic squamous cell carcinoma of the head and neck (R/M SCCHN) receiving cetuximab, fluorouracil and cisplatin alone or with docetaxel in a phase II clinical trial (CeFCiD).* Onkologie, 2012. **35**: p. 153-153.
43. Fattahi, H., et al., *Magnetoliposomes as multimodal contrast agents for molecular imaging and cancer nanotheragnostics.* Nanomedicine, 2011. **6**(3): p. 529-544.
44. Aime, S., et al., *Pushing the Sensitivity Envelope of Lanthanide-Based Magnetic Resonance Imaging (MRI) Contrast Agents for Molecular Imaging Applications.* Accounts of Chemical Research, 2009. **42**(7): p. 822-831.
45. Terreno, E., et al., *Determination of water permeability of paramagnetic liposomes of interest in MRI field.* Journal of Inorganic Biochemistry, 2008. **102**(5-6): p. 1112-1119.

46. Fossheim, S.L., et al., *Paramagnetic liposomes as MRI contrast agents: Influence of liposomal physicochemical properties on the in vitro relaxivity.* Magnetic Resonance Imaging, 1999. **17**(1): p. 83-89.
47. Castelli, D.D., et al., *Metal containing nanosized systems for MR-Molecular Imaging applications.* Coordination Chemistry Reviews, 2008. **252**(21-22): p. 2424-2443.
48. Rizzitelli, S., Giustetto, P., Boffa, C., Delli Castelli, D., Cutrin, J.C., Aime, S., Terreno, E., *In vivo MRI visualization of release from liposomes triggered by local application of pulsed low intensity non focused ultrasound.* Nanomedicine, 2014.
49. Barge, A., et al., *How to determine free Gd and free ligand in solution of Gd chelates. A technical note.* Contrast Media & Molecular Imaging, 2006. **1**(5): p. 184-188.
50. Nanni, P., et al., *TS/A: a new metastasizing cell line from a BALB/c spontaneous mammary adenocarcinoma.* Clinical & experimental metastasis, 1983. **1**(4): p. 373-80.
51. Steckner, M.C., B. Liu, and L. Ying, *A new single acquisition, two-image difference method for determining MR image SNR.* Medical Physics, 2009. **36**(2): p. 662-671.
52. Dietrich, O., et al., *Measurement of signal-to-noise ratios in MR images: Influence of multichannel coils, parallel imaging, and reconstruction filters.* Journal of Magnetic Resonance Imaging, 2007. **26**(2): p. 375-385.
53. Henkelman, R.M., *MEASUREMENT OF SIGNAL INTENSITIES IN THE PRESENCE OF NOISE IN MR IMAGES.* Medical Physics, 1985. **12**(2): p. 232-233.
54. Castellano G, B.L., Li LM, and Cendes F., *Texture analysis of medical images.* Clin Radiol, 2004. **59**(12): p. 1061-9.
55. Haralick RM, S.K., and Dinstein IH, *Textural Features for Image Classification.* Systems, Man and Cybernetics, IEEE Transactions on 1973. **SMC-3**(6): p. 610-21.
56. DA, R.A.a.J., *Quantification of histochemical staining by color deconvolution.* Anal Quant Cytol Histol 2001. **23**(4): p. 291-9.
57. Delli Castelli, D., et al., *In vivo MRI multicontrast kinetic analysis of the uptake and intracellular trafficking of paramagnetically labeled liposomes.* Journal of Controlled Release, 2010. **144**(3): p. 271-279.
58. de Smet, M., et al., *Magnetic resonance imaging of high intensity focused ultrasound mediated drug delivery from temperature-sensitive liposomes: An in vivo proof-of-concept study.* Journal of Controlled Release, 2011. **150**(1): p. 102-110.
59. S. Rizzitelli, P.G., C. Boffa, M. Ruzza, J.C. Cutrin, D. Delli Castelli, S. Aime, E. Terreno, *In vivo MRI visualization of drug release induced by non focused ultrasound in an experimental tumor model* WMIC 2012 – 5-8 September 2012 – Dublin – Ireland 2012.

Figures

Figure 1

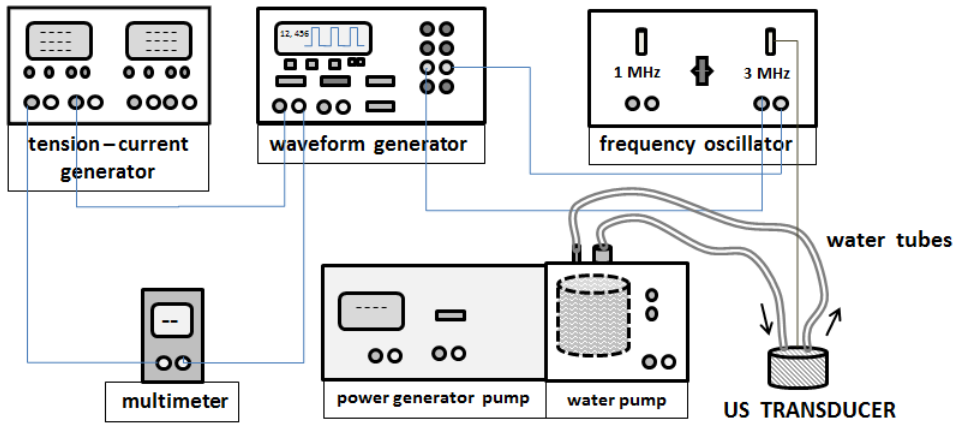

Scheme of the circuit used for the generation of pLINFU

Figure 2

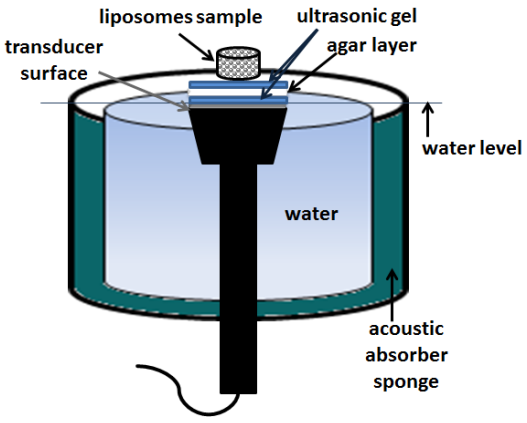

Insonation setup for *in vitro* experiments.

Figure 3

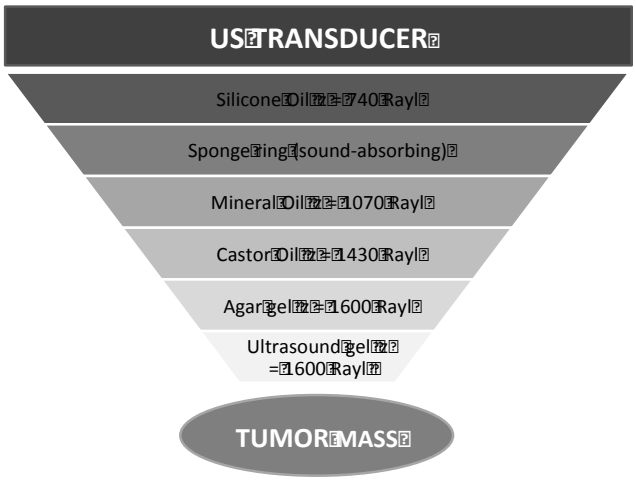

Composition of the multilayer interface used for *in vivo* experiments

Figure 4

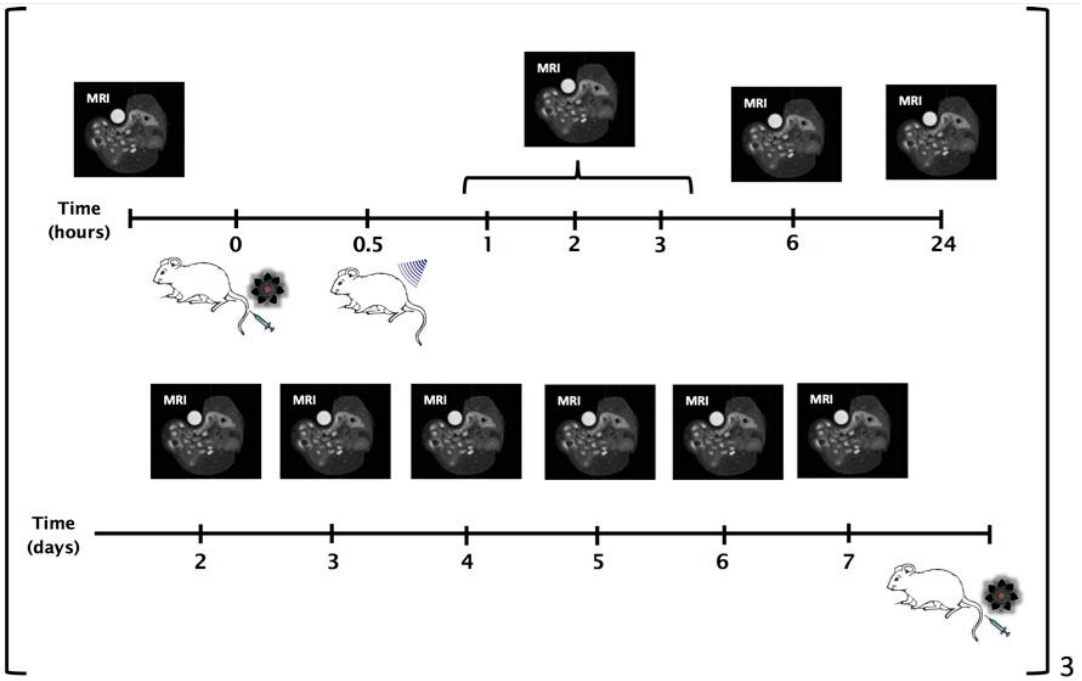

Schematic view of the experimental planning

Figure 5

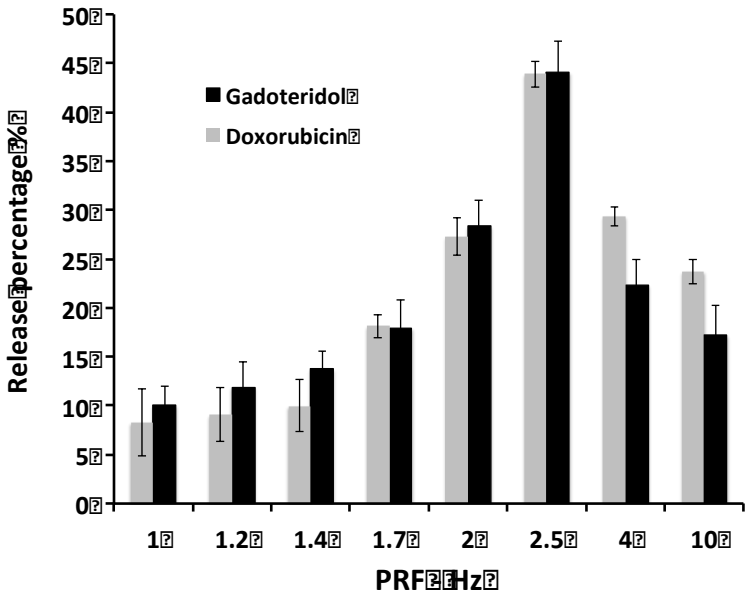

pLINFU-stimulated release of Doxorubicin and Gadoteridol from stealth liposomes *in vitro*. The release was evaluated by spectrofluorimetry (Doxorubicin) and relaxometry (Gadoteridol), respectively. Liposomes were insonated by non-focused US, total time 2 min, duty cycle 50%.

Figure 6

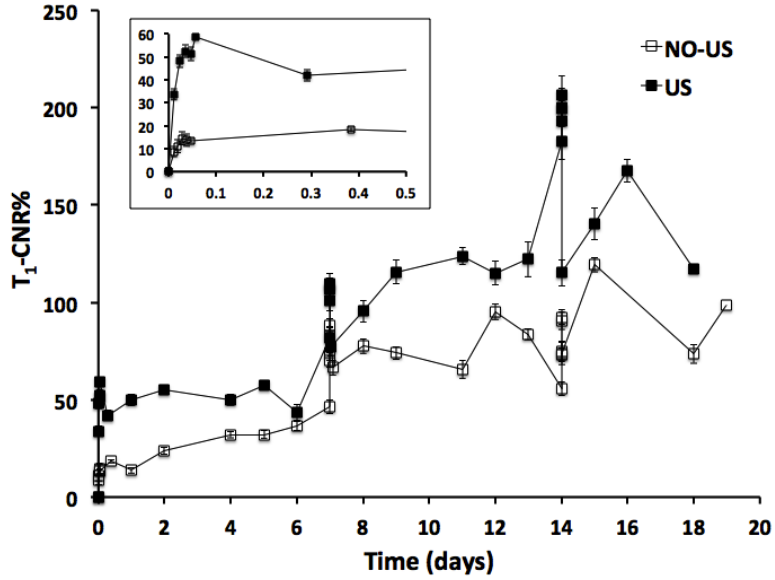

Time evolution of CNR(T_1)% measured in the tumour for US- and NoUS mice groups after injection of Gado-Doxo-Lipo. Liposomes were injected IV at days 0, 7 and 14 with a dose of 0.1 mmol/kg bw of Gadoteridol and 5 mg/kg bw of Doxorubicin. The inset shows the evolution after the first injection.

Figure 7

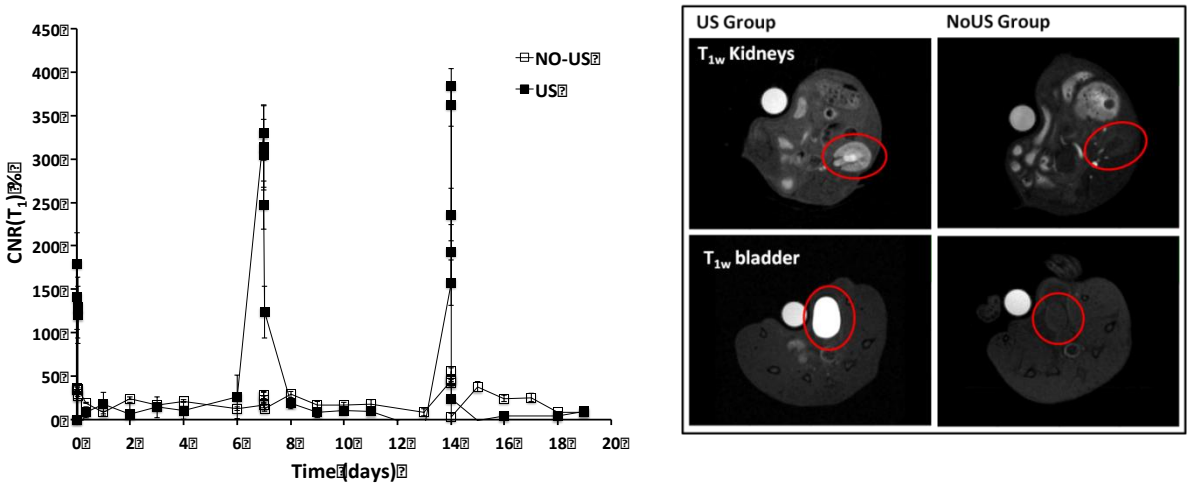

Left: temporal evolution of CNR(T_1) values measured calyx of the kidneys for US- and NoUS-groups. Right: T_{1w} MR images of kidneys (top row) and bladder (bottom row) 15 minutes after liposomes injection.

Figure 8

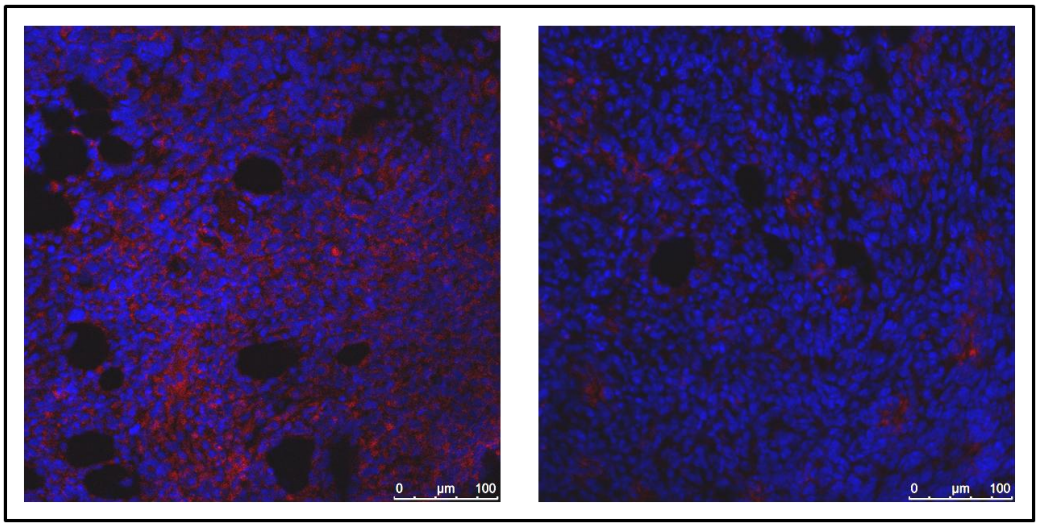

CLSM images of tumour sections from US- (left) and NoUS (right) groups explanted just after Gado-Doxo-Lipo injection. (100x, DAPI staining).

Figure 9

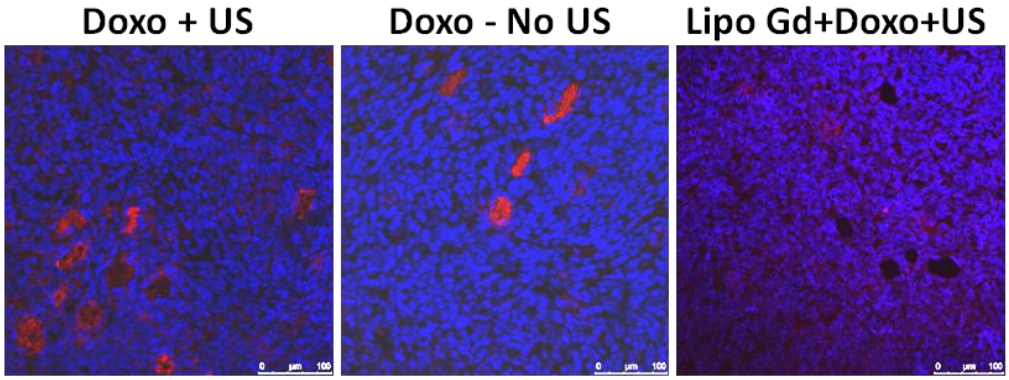

CLSM images of tumour sections of mice injected with free Doxorubicin exposed (left) or not exposed (middle) to pLINFU. Right: tumour of a mouse injected with free Doxorubicin and Gadoteridol-loaded liposomes and exposed to pLINFU. Tumours were explanted just after drug administration (100x, DAPI staining).

Figure 10

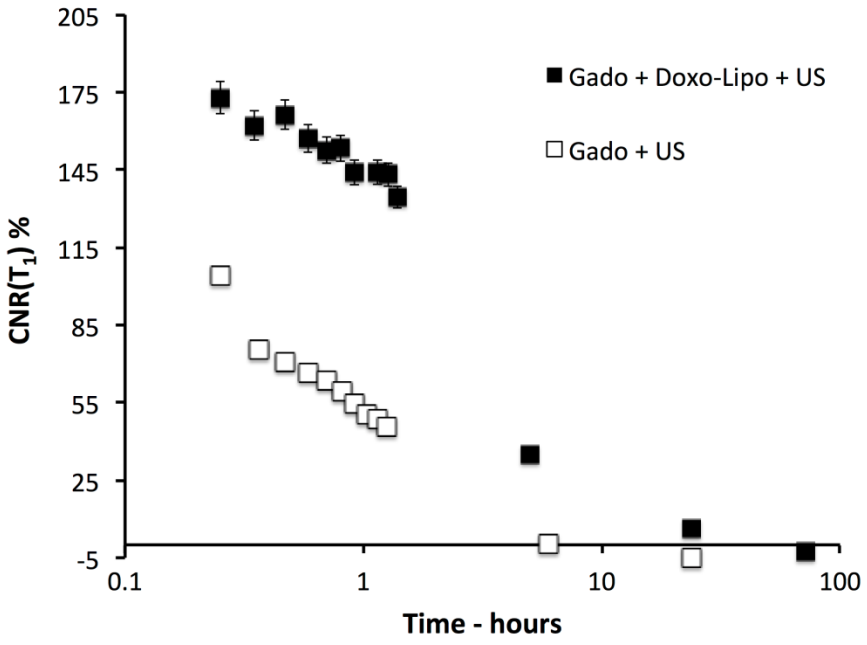

Temporal evolution of CNR(T_1) values measured in the tumor area for animals treated with free Gadoteridol in presence (filled square) or absence (open square) of liposomes, followed by pLINFU exposure.

Figure 11

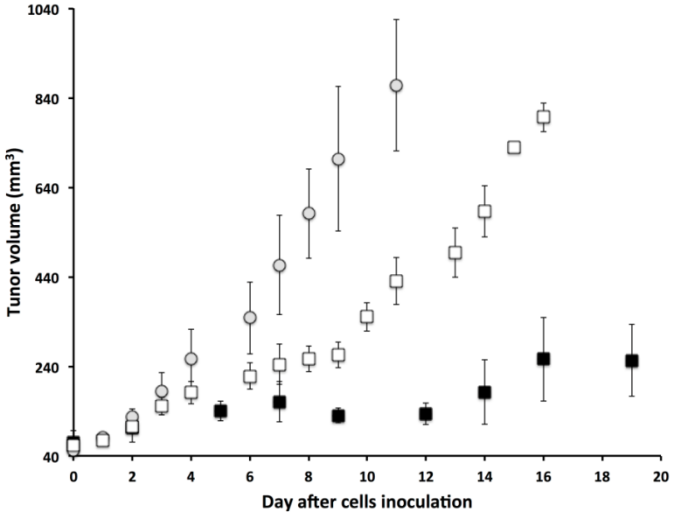

Tumour progression as a function of the time elapsed from the monitored by MRI for US-(filled square), NoUS (open square), and Control (grey filled circles) groups. Time zero corresponds to the moment in which the tumour volume was around 60 mm^3. Gado-Doxo-Liposomes were injected at days 0, 7, and 14. pLINFU stimulation (for US-group only) was carried out just after the injection.

Supplementary Material

Click here to download Supplementary Material: Supporting Material.docx